Durability assessment of soft elastomeric capacitor skin for SHM of wind turbine blades

Austin Downey, Anna Laura Pisello, Elena Fortunati, Claudia Fabiani, Francesca Luzi, et al.

Austin Downey, Anna Laura Pisello, Elena Fortunati, Claudia Fabiani, Francesca Luzi, Luigi Torre, Filippo Ubertini, Simon Laflamme, "Durability assessment of soft elastomeric capacitor skin for SHM of wind turbine blades," Proc. SPIE 10599, Nondestructive Characterization and Monitoring of Advanced Materials, Aerospace, Civil Infrastructure, and Transportation XII, 105991J (27 March 2018); doi: 10.1117/12.2296518

SPIE.

Event: SPIE Smart Structures and Materials + Nondestructive Evaluation and Health Monitoring, 2018, Denver, Colorado, United States

Durability assessment of soft elastomeric capacitor skin for SHM of wind turbine blades

Austin Downey[a,b], Anna Laura Pisello[c,d], Elena Fortunati[e], Claudia Fabiani[c], Francesca Luzi[e], Luigi Torre[e], Filippo Ubertini[e], and Simon Laflamme[b,f]

[a]Department of Mechanical Engineering Iowa State University, Ames, IA, USA
[b]Department of Civil, Construction, and Environmental Engineering, Iowa State University, Ames, IA, USA
[c]CIRIAF Interuniversity Research Centre on Pollution and Environment Mauro Felli, Perugia, Italy
[d]Department of Engineering, University of Perugia, Perugia, Italy
[e]Department of Civil and Environmental Engineering, University of Perugia, Perugia, Italy
[f]Department of Electrical and Computer Engineering, Iowa State University, Ames, IA, USA

ABSTRACT

Renewable energy production has become a key research driver during the last decade. Wind energy represents a ready technology for large-scale implementation in locations all around the world. While important research is conducted to optimize wind energy production efficiency, a critical issue consists of monitoring the structural integrity and functionality of these large structures during their operational life cycle. This paper investigates the durability of a soft elastomeric capacitor strain sensing membrane, designed for structural health monitoring of wind turbines, when exposed to aggressive environmental conditions. The sensor is a capacitor made of three thin layers of an SEBS polymer in a sandwich configuration. The inner layer is doped with titania and acts as the dielectric, while the external layers are filled with carbon black and work as the conductive plates. Here, a variety of samples, not limited to the sensor configuration but also including its dielectric layer, were fabricated and tested within an accelerated weathering chamber (QUV) by simulating thermal, humidity, and UV radiation cycles. A variety of other tests were performed in order to characterize their mechanical, thermal, and electrical performance in addition to their solar reflectance. These tests were carried out before and after the QUV exposures of 1, 7, 15, and 30 days. The tests showed that titania inclusions improved the sensor durability against weathering. These findings contribute to better understanding the field behavior of these skin sensors, while future developments will concern the analysis of the sensing properties of the skin after aging.

Keywords: Soft elastomeric capacitor, structural health monitoring, durability, titania, titanium dioxide, TiO_2, weatherability, environmental degradation

1. INTRODUCTION

Recently, the use of smart materials has seen considerable research interest for the long-term SHM of civil infrastructures.[1–5] Of particular interest is the monitoring of wind turbine systems operating in either offshore[6] or remote environments[7] where maintenance and operation costs may be from two to five times higher than for in-land systems. These smart materials have the potential to greatly improve the functionality of fully integrated SHM systems deployed on wind turbines. Potential benefits provided by these smart materials include reduced manufacturing and installation costs,[8] large area sensing capabilities[2] and fully integrated electronics.[3] Another unique feature of these smart materials is the capability to both cover large areas and, when deployed in a dense sensor network, distinguish local from global damages.[5,9] However, due to the novelty of these sensing technologies, the effect of environmental conditions on this new class of smart materials has not been sufficiently addressed. The proper design and implementation of an SHM system network must consider the environmental

Further author information: (Send correspondence to Anna Laura Pisello: E-mail:anna.pisello@unipg.it)

Nondestructive Characterization and Monitoring of Advanced Materials, Aerospace, Civil Infrastructure, and Transportation XII, edited by Peter J. Shull, Andrew L. Gyekenyesi, Tzu-Yang Yu, H. Felix Wu, Proc. of SPIE Vol. 10599, 105991J · © 2018 SPIE · CCC code: 0277-786X/18/$18 · doi: 10.1117/12.2296518

conditions that the sensor will undergo, including changes in temperature, moisture, and ultraviolet (UV) radiation. In addition, the sensing system will need to provide reliable measurements throughout the design life of the system, which is currently considered to be 10-30 years for wind turbines.[10] This study advances the applicability of smart materials through investigating the durability of a specific soft sensor developed by the authors.

The investigated sensor, termed the soft elastomeric capacitor (SEC), is a low-cost, large-area, strain-sensitive sensor.[11] When deployed in a dense sensor network configuration, the SEC is capable of detecting and localizing damage over the large area of a wind turbine blade.[5] The SEC is a parallel plate capacitor developed around a styrene-co-ethylene-co-butylene-co-styrene (SEBS) block co-polymer matrix. SEBS is selected due to its purity, elasticity, and strength.[12] TiO_2 (titania or titanium dioxide) is used to dope the dielectric layer to increase the dielectric permittivity and durability.[13,14] The dielectric is formed using a dropcast process where the sensor's dielectric mix, dissolved in toluene, is cast onto a glass plate. Once the toluene is allowed to evaporate, a conductive plate is painted onto both sides of the dielectric using an SEBS-based conductive paint made from carbon black particles. Carbon black as the conductive filler for the capacitor plates is selected for its conductivity, low-cost, simple manufacturing process, ability to absorb both UV and visible light, and its demonstrated weathering protection in plastics and polymer melt mixes.[15,16] More details regarding the fabrication of the SEC sensors can be found in the literature.[11,17]

The long-term durability of the SEC is a critical factor for its intended application to the monitoring of wind turbine blades, along with possible applications to other civil infrastructures. This work provides an assessment of the sensor's robustness under various environmental conditions where the SEC's dielectric is formulated using varying percentages of TiO_2, here 0%, 5%, 10%, and 15% by volume. The focus of this research is the development of a mechanically robust sensor that is able to withstand the thermal, humidity and UV radiation cycles that the sensor would undergo in a typical exposed application. Particularly, it is important that the capacitance of the sensor does not vary significantly with aging in order to provide consistent strain transducing capabilities. Both the sensor's dielectric and the SEC sensor itself are studied under a variety of induced environmental conditions simulated within an accelerated weathering chamber (QUV tests). These environmental conditions simulated thermal, humidity and UV radiation cycles. Once the accelerated weathering tests were completed, a series of tests were performed in order to characterize their capacitance, mechanical, thermal performance and solar reflectance at 0, 1, 7, 15, and 30 days. The key contributions of this work are a quantification of the increased durability provided by the doping of the SEBS matrix with TiO_2 and that the SEC sensors when doped with a sufficient level of TiO_2.

2. THE SOFT ELASTOMERIC CAPACITOR

The Soft Elastomeric Capacitor (SEC), shown in Figure 1, is a highly scalable thin-film strain sensor with notable elastic properties. The sensor is a parallel plate capacitor composed of three layers. These layers consist of two conductive plates and a dielectric as seen in the expanded view of the SEC in Figure 1(b). The sensor's strain sensing principle is derived from the fact that a measurable change in the capacitance of a sensor is provoked by a change in the area (i.e. strain) of the monitored surface. The SEC is adhered and pretensioned to the substrate using a commercial two-part epoxy. The fabrication of the SEC is simple and does not require any highly specialized manufacturing or processing equipment. The inner layer of an SEC, the dielectric of the capacitor, is made of an SEBS block co-polymer and filled with TiO_2 to increase both its durability and permittivity.[13,14] TiO_2 is dispersed into a mixture of SEBS and toluene using an ultrasonic tip (D100 Sonic Dismembrator manufactured by Fisher Scientific). The mixture of SEBS-TiO_2 is dropcast onto a 75×75 mm^2 glass slide covered with a non-porous Polytetrafluoroethylene (PTFE) coated fiberglass fabric. The toluene is then allowed to evaporate over 48 hours, resulting in a highly flexible thin-film dielectric. The sensors conductive plates are fabricated from a similar SEBS-toluene solution, but doped with carbon black (Printex XE 2-B) instead of TiO_2. The carbon black allows for conductive pathways to form within the SEBS matrix. This solution is hand painted onto both sides of the sensor and a copper contact is added to the sensor with a conductive adhesive. Lastly, a thin layer of the conductive paint is added on top of the copper contact to ensure a good connection between the copper contact and SEBS-based conductive paint as shown in Figure 1(a). The capacitance, C, of an SEC can be written

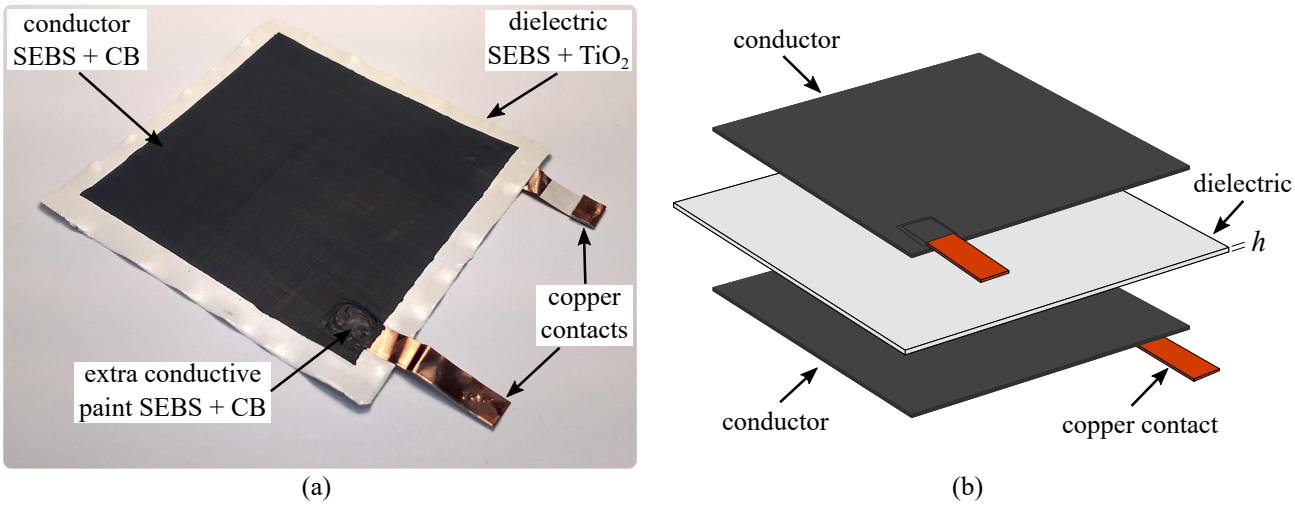

Figure 1. The soft elastomeric capacitor (SEC): (a) picture of a sensor used in this study with key components annotated; (b) an exploded view of the sensor geometry with key components annotated.

$$\Delta C = e_0 e_r \frac{\Delta A}{\Delta h} \tag{1}$$

where $e_0 = 8.854$ pF/m and e_r are the vacuum permittivity and the polymer relative permittivity, respectively. A is the overlapping area of the conductive electrodes and h is the thickness of the dielectric. The static[11] and dynamic[17] sensing capabilities of the SEC have been investigated. In addition to these material-based studies, the SEC has been experimentally investigated for structural health monitoring specific applications, including: fatigue crack detection;[9] full field strain map reconstruction;[18] and damage detection and localization in a model wind turbine blade under aerodynamic loading.[5]

3. EXPERIMENTAL METHODOLOGY

3.1 Investigated specimens

Sensor samples for this study consisted of 24 SEC sensors and 20 dielectric samples. Of the SEC sensors, eight were used for control and 15 were used as testing samples. Both the SEC sensors and the dielectric samples measured 75 × 75 mm^2 while the SEC sensors had a sensing area of 65 × 65 mm^2. This reduction in the sensors sensing area is due to the extra dielectric that extends past the end of the conductive plates, as shown in Figure 1(a). The average capacitance of the SEC sensors after fabrication, when measured as sitting flat on a table in a relaxed state, was 535 pF with a standard deviation of 30 pF. For the SEC sensors, three different percentages of TiO_2 are investigated: 5%, 10%, and 15% TiO_2 by volume. Due to difficulties in painting the SEBS-based conductive paint onto dielectric samples without TiO_2, a 0% TiO_2 sample is not considered for the SECs. Likewise, the 20 dielectric samples were fabricated with four different levels of TiO_2: 0% (pure SEBS), 5%, 10%, and 15% TiO_2 by volume. Material samples were cut from the both the SEC and dielectric samples for the mechanical testing, as needed.

3.2 Sensor weathering tests

The durability investigation of both the dielectric and SEC sensor samples was performed by means of an accelerated weathering test. This experimental investigation is used to quantify the sensors' comparative resistance capability against the combined forces of thermal stress and damaging solar radiation. The different specimens were placed in a QUV machine (QUV Accelerated Weathering Testes, Q-Lab), and the aging test was carried out following the ASTM D 4329-99,[19] linked to the operative procedure described in the ASTM G 154-06.[20] According to the standard procedure, the specimens were alternately exposed to repeated cycles of UVA radiation

(340 nm, energy of 0.77 W/m^2) at 50 °C for 8 hours, than 2 hours in a humid condition (100 RH%) at 40 °C and lastly 2 hours at 20 °C (100 RH%). The effect of the accelerated weathering tests on the different SEC and dielectric mixes was evaluated in terms of visual observations, color variation, mechanical responses by tensile test and degradation properties by thermogravimetric analysis after 1, 7, 15, and 30 days of exposure.

3.3 Mechanical and thermal characterization of the samples

Mechanical, thermal, electrical and optical characterizations were performed both before and after the exposures by means of the QUV test. The samples' mechanical behavior before and after the accelerated weathering was evaluated by failure tensile tests. Specifically, the mechanical characterization was performed using a material testing machine (Lloyd Instrument LR 30) with a 500 N load cell at room temperature on five rectangular samples (50 mm × 5 mm). An initial gauge length of 25 mm along with a crosshead speed of 100 mm/min were used during testing. From the material samples' stress-strain curves, the Young's modulus (E), the tensile strength (σ_r), and elongation at break (ε_b) were measured.

Thermal degradation, before and after the UV weathering, was evaluated by thermogravimetric analysis (TGA), using a TGA system (Seiko Exstar 6300). TGAs of the different material samples were performed using the following test parameters: 10 mg weight samples, nitrogen flow rate of 250 ml/min, and temperatures ranging from 30 °C to 800 °C with a heating rate of 10 °C/min. The residual mass from thermogravimetric curves of different mixes at different time was evaluated in order to study the effect of UV weathering on the degradation behavior of the studied materials.

3.4 Optical and visual characterization of the samples

Photographs of the different samples before and after the exposure to the UV weathering were taken for visual comparison, whereas the color changes of studied materials during weathering were examined with a spectrophotometer (CM-2300d Konica Minolta, Japan). Data was acquired using the SCI 10/D65 method with CIELAB color variables, as defined by the International Commission on Illumination.[21] The specimens were placed on a standard white plate, allowing for the and ΔL*, Δa*, and Δb* parameters and gloss level to be determined.

Optical analyses were performed by means of a solar spectrophotometer with an integrating sphere according to the international test method reported in ASTM E 903-96,[22] which describes the procedure to perform measurements of spectral near normal-hemispherical reflectance over the spectral range of 300-2500 nm with a lab instrument. For typical applications, solar reflectance values are usually calculated by weighting wavelength with respect to reference solar spectra, according to reference values.[23] In this study, given the focus on the material characterization and not specifically on its capability to stay cooler under the solar radiation, a simple measurement technique is implemented and terrestrial solar irradiance distribution is not evaluated. The spectrophotometer used (SolidSpec-3700) is equipped with a 60 mm-diameter integrating sphere and has a wavelength accuracy of 0.1 nm. The machine functions with a double beam scheme and coated optics. The measurement procedure started by recording the spectral 100% and the zero lines to be kept as reference for the whole characterization campaign. Then, all materials were tested and the reflectance values were obtained similar to other literature work,[24] as reported in the following sections.

3.5 Electrical characterization of the samples

The capacitance of SEC sensors after aging was measured and compared to the capacitance of the sensor after manufacturing to investigate their durability. Capacitance was measured using an LCR meter (875B manufactured by BK precision). First, the eight control sensors were considered and their capacitance was measured after fabrication and again after one year without any accelerated aging. During this year, the sensors were left in a laboratory environment at room temperature. The capacitance for the 15 SEC samples used for the durability investigation was measured. These measurements were also taken after 1 year with sensors being subjected to either 0, 1, 7, 15, and 30 days of QUV aging. Due to the fact that materials were cut from each of these samples, as required by the material testing needs, the capacitance of portions of the sensors was measured (e.g. a 35 × 75 mm^2) and adjusted through Equation 1. This adjustment was based on the change in area caused by the removed material to obtain an estimated capacitance for the sensors after aging.

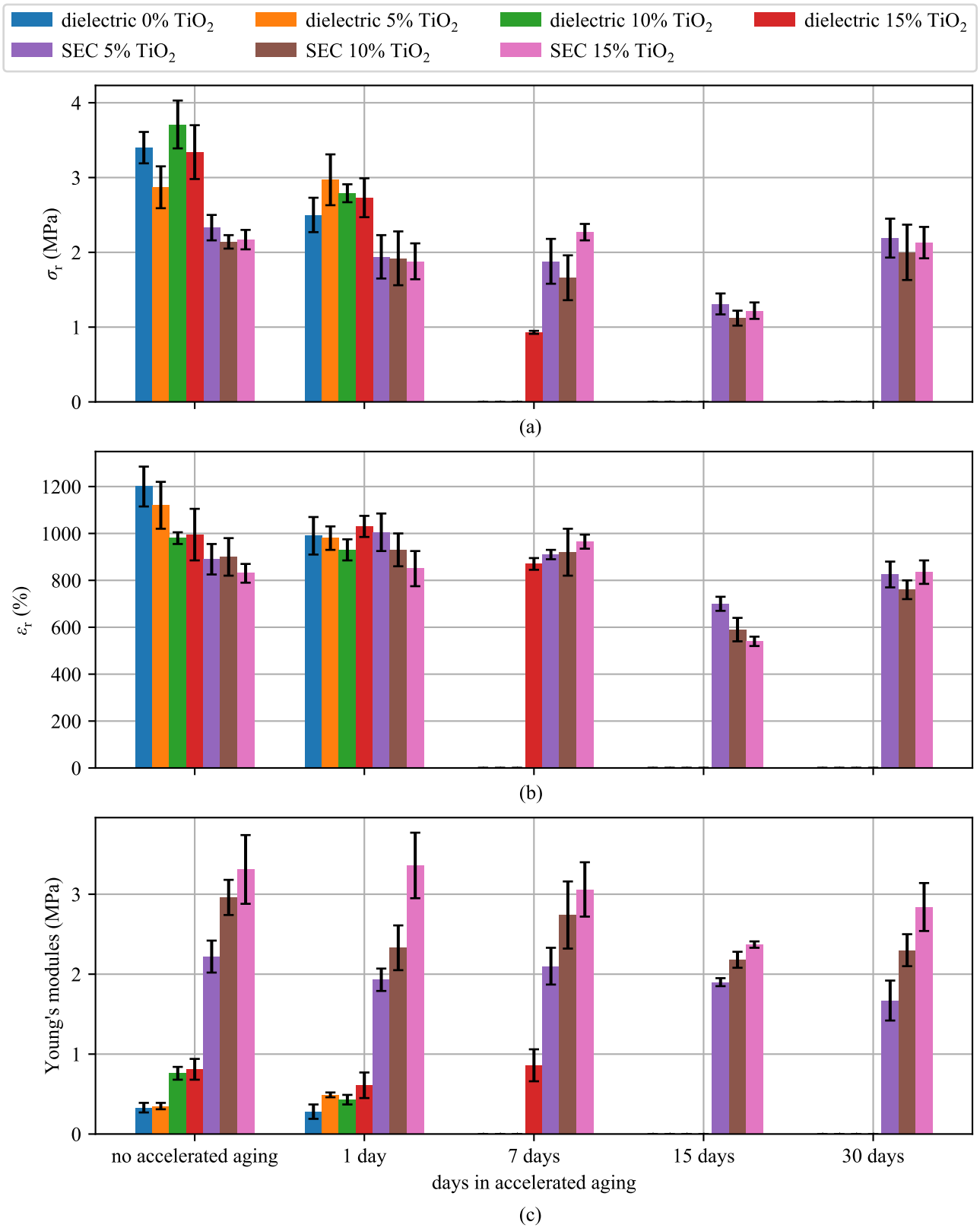

Figure 2. Mechanical properties of the SECs and dielectrics, with different levels of TiO_2 (dielectric layer), after accelerated aging: (a) tensile strength; (b) elongation at break; (c) Young's modulus.

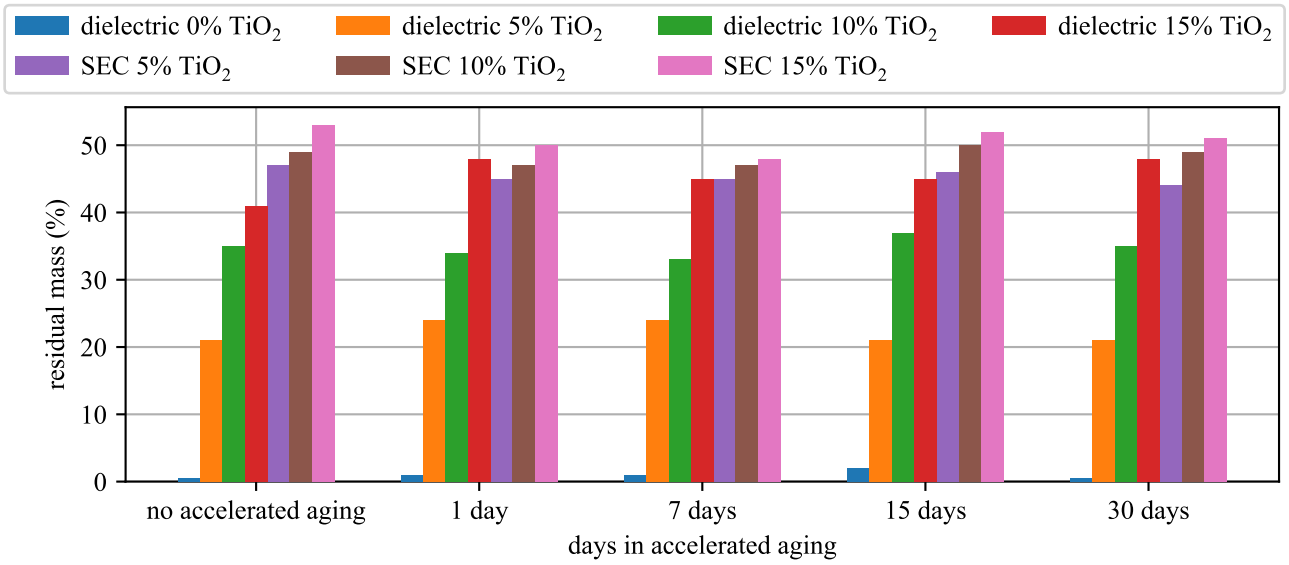

Figure 3. Residual masses of the SECs and dielectrics, with different levels of TiO_2 doped into the dielectric layer, after accelerated aging.

4. RESULTS AND DISCUSSION

4.1 Durability analysis of mechanical and thermal behavior of the samples

The effect of the accelerated weathering test performed on the different sensors and dielectrics was evaluated in terms of visual observations, color variation, mechanical responses by tensile test and degradation properties by thermogravimetric analysis after 1, 7, 15, and 30 days of exposure, using a QUV machine and considering 12-hour long thermal cycles. Each cycle consisted of temperature variations from 20 °C to 50 °C with a UV intensity value of 0.77 W/m^2 at 340 nm of wavelength.

Figure 2 shows the mechanical properties of SECs and dielectric layers after accelerated aging under various levels of TiO_2 in the dielectric layer. Results show that the pure dielectric (0% TiO_2) is quite sensitive to aging, with tensile strength and elongation at break exhibiting notable reductions after just one day of accelerated aging. The addition of TiO_2 is seen to highly improve the dielectric's durability, which is particularly observable with the elongation at break. The carbon-black-based conductive layer found over the SECs results in stable mechanical properties even after 30 days of accelerated aging. It is also found that the inclusion of TiO_2 increases the Young's modulus of the SEC.

Values of the residual masses of the samples after accelerated aging are shown in Figure 3. The dielectric and sensor samples with higher levels of TiO_2 retained more residual mass relative to samples with lower levels of TiO_2. This is clearly observable for the dielectric layer, where the dielectric with 15% TiO_2 retained more than 40% of its mass while the dielectric with 0% TiO_2 retained about 1% of its mass. Aging does not appear to influence the residual mass of any sample.

4.2 Optical and visual analysis

Results from the spectrophotometer analysis, as presented in Figure 4, can be used to investigate the durability of the membranes in terms of solar reflectance variation due to the weathering procedure. Figure 4 shows the relative differences between the total reflectance of the reference membranes, i.e. the dielectric layer and the SEC sensors, and the same samples exposed to 1, 7, 15, and 30 days of aging, using the accelerated weathering test. In general, results indicate a significantly better behavior of the SEC samples compared to the dielectrics. As observed in the left column of Figure 4, only the 1 day aged dielectric samples could be tested for each of the four TiO_2 concentration values, while the samples exposed to a 7 days-long weathering could only be analyzed when 10 and 15% TiO_2 was added to the dielectric membrane. Higher exposure time caused such a high level

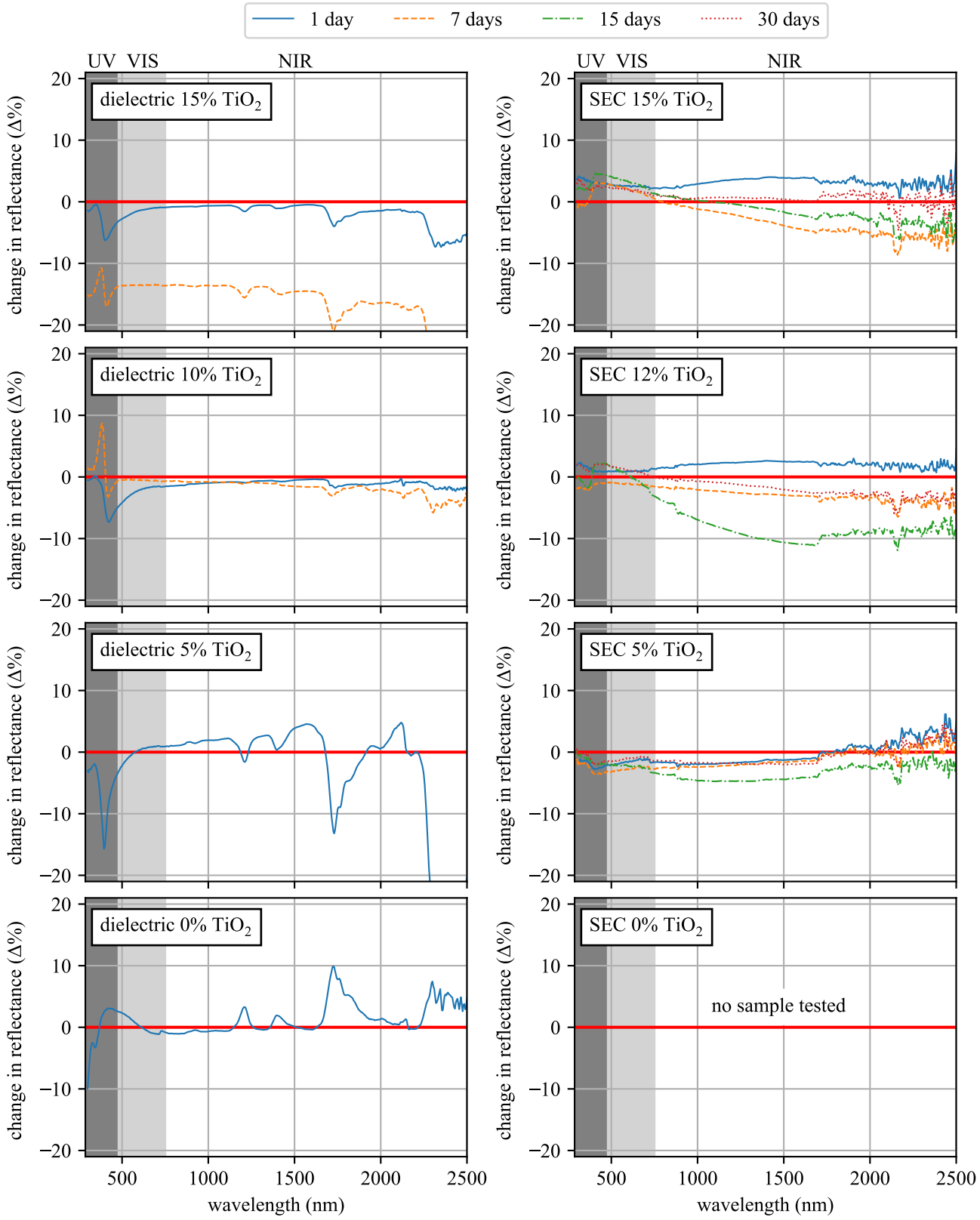

Figure 4. Change in solar reflectance of the dielectric and the SEC sensor exposed to 1, 7, 15, and 30 days of weathering procedure with respect to the same reference samples, e.g. the dielectric and of the SEC sensors with 0 days of aging $(SR_{day} - SR_{day-0}) / SR_{day-0}$.

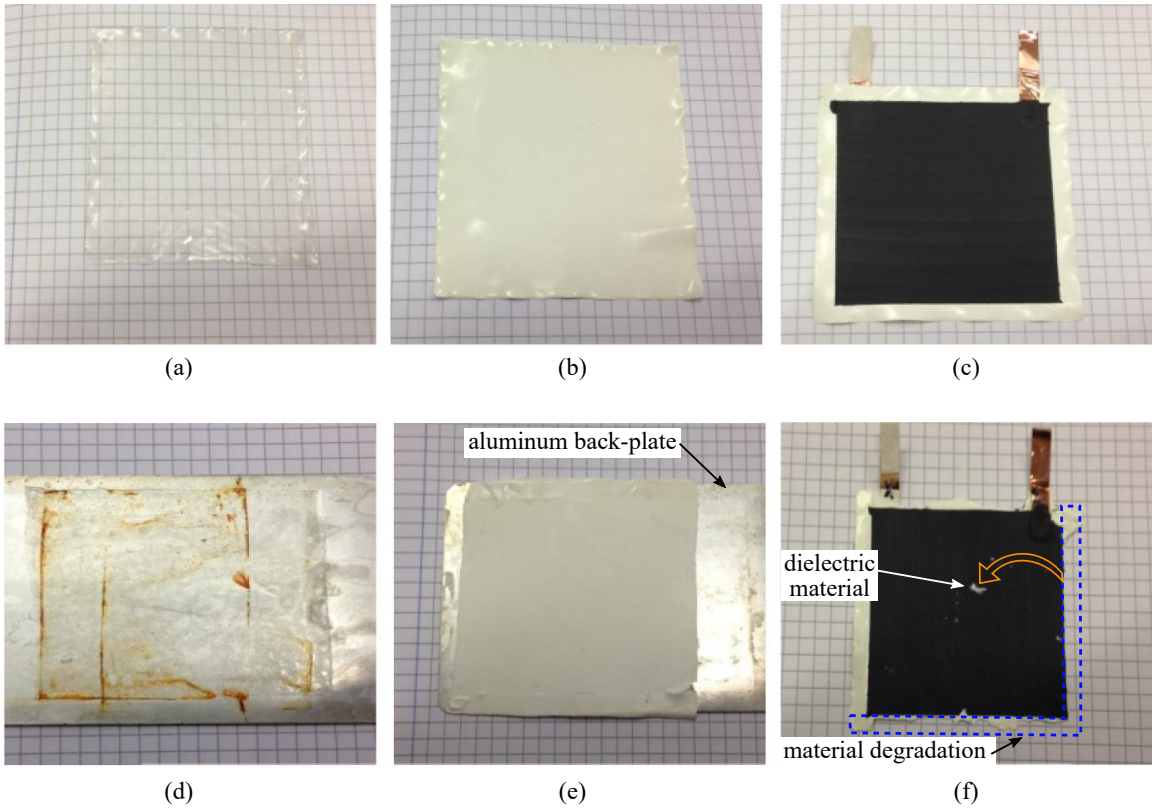

Figure 5. (a-f): A dielectric with 0% TiO_2, a dielectric with 15% TiO_2, and an SEC with 15% TiO_2 before (a-c) and after (d-f) the QUV test, respectively. Subfigure (f) shows the deposition of the dielectric material on top of the conductive layer.

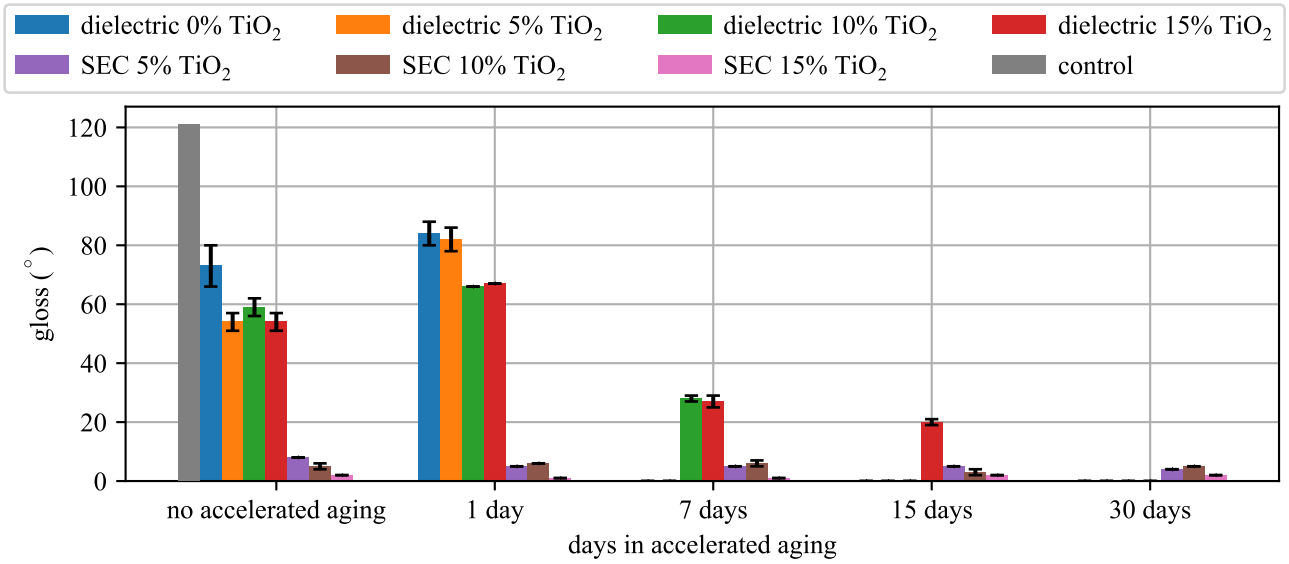

Figure 6. Colorimetry analysis of SECs and dielectrics with different levels of TiO_2 in the dielectric layer, after accelerated aging.

Table 1. Initial capacitance of control specimens and its variation after 12 months.

sensor no.	TiO_2 (%)	initial C (pF)	final C (pF)	change (%)
1	5	497	499	0.40
2	5	535	540	0.93
3	5	516	523	1.36
4	10	549	554	0.91
5	10	576	574	-0.35
6	10	537	545	1.49
7	15	528	527	-0.19
8	15	574	566	-1.39

of damage to the dielectric samples that it was not possible to perform any spectral analysis on them. The SEC samples, as shown in the right column of Figure 4, appear to be more resilient to the accelerated aging tests. Although they were exposed to the same weathering cycles as the dielectrics, they all retained a level of mechanical stability that allowed spectrophotometer testing. In this case, despite the lower relative difference between the reference and the other samples, i.e. below $\pm$ 10% vs values higher than 12% for the dielectric samples, it is interesting to note that the addition of titanium dioxide to the original mixture seems to produce a higher spectral variation in the samples, particularly in the near infrared region (NIR) of the spectrum. However, the highest variations are generally associated to the samples exposed to a 1 and 15 days-long weathering cycle, while after 30 days all of the samples show a reduced relative difference with respect to the neat sample. Lastly, the introduction of carbon black seems to produce a highly scattered behavior in the range 1700-2500 nm.

Pictures of samples after fabrication and after 30 days of accelerated weathering tests are shown in Figure 5. These photographs show the degradation for the dielectric layer with 0% TiO_2 before (5(a)) and after (5(d)) aging. In the case of the dielectric layer after aging, the material was too fragile to be remove from the aluminum back-plate, which explains the view of the back-plate in the picture. The oxidation in Figure (5(d)) came from other materials not part of this current study that were tested in close proximity to the sample in the QUV chamber. In comparison, the dielectric layer doped with 15% TiO_2 exhibits only a limited difference from before (Figure 5(b)) and after (Figure 5(e)) aging. Figures 5(c) and 5(f) present the effects of 30 days of accelerated aging on an SEC sensor with a dielectric that is doped with 15% TiO_2. The unprotected portions of the dielectric layer around the outside of the SEC sensor did degrade, and once fully separated some pieces of the dielectric layer fell onto the carbon-black-based conductor as denoted by the arrow in Figure 5(f). No holes were found in the conductor layer of the SEC sensors. The conductive layer was found to provide an excellent protective layer for the dielectric.

Results of the colorimetry analysis are shown in Figure 6. Quantitatively, these results confirm that the color of the dielectric with 15% TiO_2 is the most stable, at least until the 15 days in the QUV chamber. Additionally, the color of the SECs undergoes limited variations with aging owing to the protection provided by the conductive plates. This data helps to further validate the stability provided by the carbon-black-based conductive plates to the accelerated weathering tests performed in this work.

4.3 Capacitance stability investigation

The capacitance values for the SEC sensors over the one year investigation period are listed in Tables 1 and 2. The aged control sensors (Table 1) do not exhibit any clear reduction in capacitance. Each sensor exhibits changes in capacitance after one year of less than 1.5 % of its initial value. Due to the sensor being allowed to sit freely on the bench during testing, this value is well within the accuracy of the measurement system. As presented in Table 2, the aged samples exhibit higher variations in their capacitance change over the 1 year period. These variations are not correlated to the number of days the samples spend in the QUV test chamber. For example, the highest variations in capacitance are found in the samples that spent only 1 day in the QUV test chamber and these samples exhibit both positive and negative changes in capacitance. These higher variations in capacitance can be attributed to the extrapolating of the capacitance values from the cut sensor samples rather than the aging of the sensors. This hypothesis is further validated by the fact that when considering the sensors

Table 2. Capacitance of SECs after QUV testing.

	sensor no.	TiO_2 (%)	initial C (pF)	final C (pF)	change (%)
No QUV	1	5	520	513	-1.44
	2	10	583	563	-3.52
	3	15	540	525	-2.78
QUV 1 day	4	5	534	624	16.85
	5	10	581	510	-12.22
	6	15	545	534	-2.02
QUV 7 days	7	5	505	540	6.93
	8	10	586	558	-4.78
	9	15	558	550	-1.43
QUV 15 days	10	5	503	486	0.91
	11	10	546	568	4.03
	12	15	507	496	-2.17
QUV 50 days	13	5	481	482	0.21
	14	10	524	504	-3.82
	15	15	487	460	-5.54

in the aged sample set, the total change for the average capacitance for all 15 sensors is a decrease of just 0.72% from their initial average capacitance.

5. CONCLUSION

The paper has investigated long-term durability of the soft elastomeric capacitor, a skin-type strain sensor developed for measuring strain over large structural surfaces. This sensor is designed as a parallel plate capacitor with the dielectric made of a styrene-co-ethylene-co-butylene-co-styrene (SEBS) block co-polymer matrix doped with TiO_2 and two conductive plates consisting of the same SEBS matrix, but filled with carbon black to increase its conductivity. The results have shown that the introduction of TiO_2 can strongly improve the durability of the inner dielectric layer of the sensor. Furthermore, the conductive plates doped with carbon black are observed to effectively act as protective layers for the inner dielectric. The increase in durability of both the SEC sensor and its dielectric layer was quantified through a series of mechanical, thermal, and optical tests. Additionally, within the constraints of this study, it was demonstrated that the capacitance of the sensor does not significantly vary through aging. Future work will include an investigation of the strain-sensitivity of the sensors under various static and dynamic loading cases. From the results presented in this research, it can be concluded that the mechanical and electrical robustness of the SEC sensor, when the dielectric is doped with at least 5% TiO_2, is resilient to the effects of accelerated weathering.

ACKNOWLEDGMENTS

The support of the National Science Foundation Grant No. 1069283, which supports the activities of the Integrative Graduate Education and Research Traineeship (IGERT) in Wind Energy Science, Engineering and Policy (WESEP) at Iowa State University is gratefully acknowledged. This work is also partly supported by the Italian Ministry of Education, University and Research (MIUR) through the funded Project of Relevant National Interest (PRIN) entitled "SMART-BRICK: Novel strain-sensing nano-composite clay brick enabling self-monitoring masonry structures" (protocol no. 2015MS5L27). Any opinions, findings, and conclusions or recommendations expressed in this material are those of the authors and do not necessarily reflect the views of the funding agencies (National Science Foundation and MIUR).

REFERENCES

[1] Kang, I., Schulz, M. J., Kim, J. H., Shanov, V., and Shi, D., "A carbon nanotube strain sensor for structural health monitoring," *Smart Materials and Structures* **15**, 737–748 (apr 2006).

[2] Loh, K. J., Hou, T.-C., Lynch, J. P., and Kotov, N. A., "Carbon nanotube sensing skins for spatial strain and impact damage identification," *Journal of Nondestructive Evaluation* **28**, 9–25 (mar 2009).

[3] Burton, A., Lynch, J., Kurata, M., and Law, K., "Fully integrated carbon nanotube composite thin film strain sensors on flexible substrates for structural health monitoring," *Smart Materials and Structures* **26**(9) (2017).

[4] Schulz, M. J. and Sundaresan, M. J., [*Smart Sensor System for Structural Condition Monitoring of Wind Turbines: May 30, 2002-April 30, 2006*], National Renewable Energy Laboratory (2006).

[5] Downey, A., Laflamme, S., and Ubertini, F., "Experimental wind tunnel study of a smart sensing skin for condition evaluation of a wind turbine blade," *Smart Materials and Structures* (Oct 2017).

[6] Kaldellis, J. and Kapsali, M., "Shifting towards offshore wind energy—recent activity and future development," *Energy Policy* **53**, 136–148 (feb 2013).

[7] Shaahid, S. and El-Amin, I., "Techno-economic evaluation of off-grid hybrid photovoltaic–diesel–battery power systems for rural electrification in saudi arabia—a way forward for sustainable development," *Renewable and Sustainable Energy Reviews* **13**, 625–633 (apr 2009).

[8] Luo, S., Hoang, P. T., and Liu, T., "Direct laser writing for creating porous graphitic structures and their use for flexible and highly sensitive sensor and sensor arrays," *Carbon* **96**, 522–531 (jan 2016).

[9] Kong, X., Li, J., Collins, W., Bennett, C., Laflamme, S., and Jo, H., "A large-area strain sensing technology for monitoring fatigue cracks in steel bridges," *Smart Materials and Structures* **26**, 085024 (jul 2017).

[10] Marín, J., Barroso, A., París, F., and Cañas, J., "Study of damage and repair of blades of a 300kw wind turbine," *Energy* **33**, 1068–1083 (jul 2008).

[11] Laflamme, S., Kollosche, M., Connor, J. J., and Kofod, G., "Robust flexible capacitive surface sensor for structural health monitoring applications," *Journal of Engineering Mechanics* **139**, 879–885 (jul 2013).

[12] Yao, Y., Tung, S.-T. E., and Glisic, B., "Crack detection and characterization techniques-an overview," *Structural Control and Health Monitoring* **21**, 1387–1413 (mar 2014).

[13] Stoyanov, H., Kollosche, M., McCarthy, D. N., and Kofod, G., "Molecular composites with enhanced energy density for electroactive polymers," *Journal of Materials Chemistry* **20**(35), 7558 (2010).

[14] Day, R., "The role of titanium dioxide pigments in the degradation and stabilisation of polymers in the plastics industry," *Polymer Degradation and Stability* **29**, 73–92 (jan 1990).

[15] "Carbon black," in [*Kirk-Othmer Encyclopedia of Chemical Technology*], Inc, J. W. &. S., ed., John Wiley & Sons, Inc. (dec 2000).

[16] Rwei, S.-P., Manas-Zloczower, I., and Feke, D. L., "Analysis of dispersion of carbon black in polymeric melts and its effect on compound properties," *Polymer Engineering and Science* **32**, 130–135 (jan 1992).

[17] Laflamme, S., Ubertini, F., Saleem, H., D'Alessandro, A., Downey, A., Ceylan, H., and Materazzi, A. L., "Dynamic characterization of a soft elastomeric capacitor for structural health monitoring," *Journal of Structural Engineering* **141**, 04014186 (aug 2015).

[18] Downey, A., Laflamme, S., and Ubertini, F., "Reconstruction of in-plane strain maps using hybrid dense sensor network composed of sensing skin," *Measurement Science and Technology* **27**, 124016 (nov 2016).

[19] "Practice for fluorescent ultraviolet (UV) lamp apparatus exposure of plastics."

[20] "Practice for operating fluorescent ultraviolet (UV) lamp apparatus for exposure of nonmetallic materials."

[21] Witt, K., "Cie guidelines for coordinated future work on industrial colour-difference evaluation," *Color Research & Application* **20**, 399–403 (dec 1995).

[22] "Test method for solar absorptance, reflectance, and transmittance of materials using integrating spheres."

[23] "Tables for reference solar spectral irradiances: Direct normal and hemispherical on 37 tilted surface."

[24] Pisello, A., "Experimental analysis of cool traditional solar shading systems for residential buildings," *Energies* **8**, 2197–2210 (mar 2015).